Dyes and Pigments 132 (2016) 110–120

Contents lists available at ScienceDirect

Dyes and Pigments

journal homepage: www.elsevier.com/locate/dyepig

# Synthesis and characterization of novel dendritic compounds bearing a porphyrin core and cholic acid units using "click chemistry"

Edgar Aguilar-Ortíz [a], Nicolas Lévaray [b], Mireille Vonlanthen [a], Eric G. Morales-Espinoza [a], Yareli Rojas-Aguirre [c], Xiao Xia Zhu [b, **], Ernesto Rivera [a, *]

[a] Instituto de Investigaciones en Materiales, Universidad Nacional Autónoma de México, Circuito Exterior Ciudad Universitaria, CP 04510, Mexico City, Mexico
[b] Département de Chimie, Université de Montréal, CP 6128, Succursale Centre-ville, Montréal, QC, H3C 3J7, Canada
[c] Facultad de Química, Universidad Nacional Autónoma de México, Circuito Exterior Ciudad Universitaria, CP 04510, Mexico City, Mexico

ARTICLE INFO

*Article history:*
Received 16 February 2016
Received in revised form
19 April 2016
Accepted 26 April 2016
Available online 27 April 2016

*Keywords:*
Porphyrin
Cholic acid
Click chemistry
Optical properties
Aggregation

ABSTRACT

Four novel dendritic molecules bearing a porphyrin core and peripheral cholic acid units (***TPPh(Zn) Tetra-CA***, ***TPPh(2H) Tetra-CA***, ***TPPh(Zn) Octa-CA and TPPh(2H) Octa-CA***) have been synthesized by the "click chemistry" approach, using azide-alkyne couplings. These compounds are fully characterized by $^{1}H$ and $^{13}C$ NMR spectroscopy and MALDI-TOF. The optical properties of the dendronized porphyrins are studied by absorption and fluorescence spectroscopy in different solvents, in order to study the amphiphilic properties of the cholic acid units in combination with the optical response of the porphyrin unit. After complexation with Zn, the metallated porphyrins (***TPPh(Zn) tetra-CA and TPPh(Zn) octa-CA***) tend to form J-aggregates in solvents of different polarity, whereas the free base porphyrins ***TPPh(2H) tetra-CA*** and ***TPPh(2H) octa-CA*** behaved differently. The aggregation phenomenon has been investigated by varying the polarity of the environment, temperature and metallation.



## 1. Introduction

Porphyrins are macrocyclic molecules which attracted much attention from researchers due to their importance in both natural and artificial chemical and biochemical systems. From the biological perspective, some classes of porphyrins and their metallic complexes play a key role in essential biological processes such as oxygen transport and photosynthesis [1,2]. In the fields of chemistry and materials science, they have been widely studied due to their vast range of potential applications including catalysis, electrocatalysis and photodynamic therapy when they are used as building blocks to engineer light-responsive systems. Of special interest are the nonlinear optical properties of the porphyrin aggregates for energy transfer to design artificial photosynthetic systems, molecular photonic wires and multiporphyrin arrays as artificial light-harvesting antennas [3–5].

The chemical modifications at their *meso* positions and the coordination chemistry either at the tetrapyrrolic core or the periphery give rise to a large number of porphyrin derivatives with unique optical and electronic features. A variety of ligands have been used to functionalize the porphyrin core, i.e., crown ethers, phosphines and pyridines to name a few [1,5]. Moreover, the porphyrin unit has been used as a core to design and synthesize novel dendritic systems. In this case, the optoelectronic properties can be tuned by modifying the structure of the dendrons, thus extending the potential of porphyrin applications [6,7]. The fascinating optical and electrochemical features of the porphyrin dendrimers have inspired us to continue exploring them. We have been working on the construction of dendritic systems by attaching branches of different architectures to the porphyrin periphery. Very recently, we reported the synthesis, photophysical and electrochemical properties of pyrene-dendronized porphyrins in order to investigate the energy transfer (FRET) mechanisms in these systems [8–10]. The interesting outcomes of this work motivated us to continue exploring the optical and photophysical properties of different dendritic porphyrin constructs, as well as the FRET phenomena which occur in them.

On the other hand, the steroid scaffold is a large and rigid non-conjugated structure prone to a variety of chemical modifications to

* Corresponding author.
** Corresponding author.
*E-mail addresses:* julian.zhu@umontreal.ca (X.X. Zhu), riverage@unam.mx (E. Rivera).

http://dx.doi.org/10.1016/j.dyepig.2016.04.047
0143-7208/

generate derivatives with a well-defined architecture. These compounds are suitable for the binding of polar species and therefore may be potentially used in anion sensing [11]. In a previous work, Vollmer and co-workers reported an energy transfer system based on a bithienylporphyrin and an anthrylthiophene unit linked via a rigid androstene bridge with the aim to investigate the influence of distance, orientation and electronic communication between the chromophores in intramolecular FRET processes. They found that the steroid nucleus partially interrupted the energy transfer and that may influence the parameters governing the efficiency of Förster-type FRET, which was assumed to be the most relevant transfer mechanism within the system [12]. These findings encouraged us to construct dendritic systems by attaching steroidal nuclei to a porphyrin unit. Several synthetic routes can be used to synthesize the porphyrinic dendrimers. The click reactions, namely the copper (I)-catalysed 1,3-dipolar cycloaddition of azides and terminal alkynes, produce in a regioselective manner the 1,4-disubstituted 1,2,3-triazole products in high yields [13]. Since the 1,2,3-triazole group has a significant performance as a π-conjugated linker in intramolecular energy transfer processes [14,15], we employed the click chemistry approach to link the cholic acid units to the porphyrin core.

On the other hand, aggregation has been widely studied in porphyrins, where H and J aggregates have been observed [16–23]. Particularly J-aggregates have a bright future in nanophotonics, since they could operate in molecular plasmonic devices, where they can feed nanostructures with absorbed light energy or serve as self-assembled optical microcavities [23,24]. Many studies about the formation of J-aggregates in porphyrins have been carried out by different research groups focussing on applications such as pH sensors, luminescence, electro and photoactivity [25–35].

In this work, we report for the first time novel dendritic porphyrins bearing cholic acid at the periphery and the study of their optical and photophysical properties in terms of the *meso*-spacer and the porphyrinic core. In addition, the aggregation phenomenon was studied under different conditions in order to study the effects of the following conditions on the self-assembly processes: polarity of the solvent, presence of the triazole units, metallation of the porphyrin and temperature.

## 2. Experimental part

### 2.1. Equipment

$^1$H and $^{13}$C NMR spectra of all compounds involved in the synthesis were recorded on a Bruker Avance 400 MHz, operating at 400 and 100 MHz, for $^1$H and $^{13}$C, respectively, in $CDCl_4$, $MeOD_4$ or $d_6$-DMSO solution. The assignments of the signals are illustrated in the Supporting Information (SI).

Absorbance spectra of the dendritic compounds were recorded on a Cary Series UV vis NIR Spectrophotometer (Agilent Technologies) using quartz cells with a width of 1 cm, employing THF, hexane and $CHCl_3$ spectrometric grade as solvent. Fluorescence spectra were recorded at room temperature on a Varian fluorescence spectrophotometer with a Xe-900 lamp exciting at 420 nm; excitation and in both cases the emission slit widths were of 5 nm. MALDI-TOF mass spectra were obtained using dithranol as matrix, on a Bruker Daltonic Felx Analysis.

### 2.2. Reagents

All reagents employed in the synthesis were purchased from Sigma–Aldrich and used without further purification. The solvents used in reactions were dried and purified by distillation and conventional methods.

### 2.3. Synthesis of the dendritic molecules

#### 2.3.1. Synthesis of 4-(prop-2-1-yloxy)benzaldehyde **(1)**

4-hydroxybenzaldehyde (5 g, 40 mmol) and propargyl bromide (3.6 mL, 40 mmol) were reacted, with $K_2CO_3$ (8.28 g, 60 mmol) as base and dry acetone (50 mL) as solvent, heating at 60 °C for 24 h (Fig. 1). The crude product was filtered and purified by column chromatography using a mixture of hexanes: ethyl acetate (9:1) to give the desired product **(1)**, which was isolated as a pale yellow solid (5.18 g, 32.3 mmol). Yield: 80%.

$^1$H NMR (400 MHz $CDCl_3$) (SI-Scheme 1) $\delta$ (ppm): 9.90 (s, 1H), 7.89–7.82 (m, 2H), 7.12–7.06 (m, 2H), 4.78 (d, $J$ = 2.42 Hz, 2H), 2.57 (t, $J$ = 2.40, 2.40 Hz, 1H).

#### 2.3.2. Synthesis of 4-((3,5-bis(prop-2-yn-1-yloxy)benzyl)oxy) benzaldehyde **(3)**

4-((3,5-bis(prop-2-yn-1-yloxy)benzyl)oxy)benzaldehyde **(3)** was obtained by a multistep Williamson etherification reaction. First, 3,5-hydroxibenzylalcohol (5 g, 36 mmol) and propargyl bromide (8 mL, 89 mmol) were reacted in dry acetone (50 mL) at 60 °C for 24 h. The crude product was purified by column chromatography to yield **(2)** as a pale yellow solid. Secondly, an Appel reaction was performed to give the corresponding alkyl bromide. This intermediate (1.68 g, 6.02 mmol) was further coupled in the presence of 4-hydroxybenzaldehyde (0.74 g, 6.02 mmol), using $K_2CO_3$ (3.32 g, 2.4 mmol) as base in dry acetone (50 mL) at 60 °C for 24 h (Fig. 1). The crude product was purified by column chromatography using a mixture of hexane: $CHCl_3$ (3:7) as eluent to give the desired product **(3)** as a pale yellow solid (1.41 g, 4.4 mmol). Yield: 73%.

$^1$H NMR (400 MHz, $CDCl_3$) (SI-Scheme 2) $\delta$ (ppm) = 2.69–2.64 (m, 2H), 4.81 (d, $J$ = 2.37 Hz, 4H), 5.23 (s, 2H), 6.72 (t, $J$ = 2.21, 2.21 Hz, 1H), 6.82 (d, $J$ = 2.17 Hz, 2H), 7.96 (d, $J$ = 8.71 Hz, 2H), 7.19 (d, $J$ = 8.69 Hz, 2H), 10.01 (s, 1H).

#### 2.3.3. Synthesis of the porphyrin core

*TPPh (2H) tetra-alkyne* **(4)** was obtained using the Lindsey method (Fig. 2) [36], which has been already reported in the literature. Pyrrole (0.495 mL, 7.1 mmol) and 4-(prop-2-1-yloxy)benzaldehyde **(1)** (1.13 g, 7.1 mmol) were dissolved in dry $CH_2Cl_2$ (31 mL); after 10 min of stirring $BF_3OEt_2$ (0.03835 mL, 0.71 mmol) was added to the solution. Then, DDQ was added (0.709 g, 7.1 mmol) to the reaction mixture in order to achieve the oxidation reaction. The crude product was purified by column

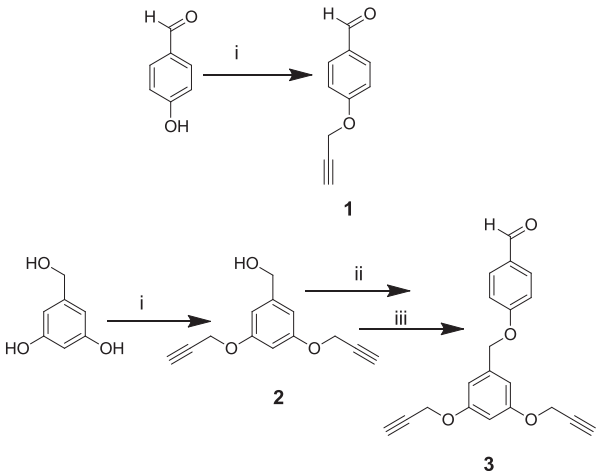


**Fig. 1.** Synthesis of *4-(prop-2-1-yloxy)benzaldehyde* **(1)** and *4-((3,5-bis(prop-2-yn-1-yloxy)benzyl)oxy)benzaldehyde* **(3)**.

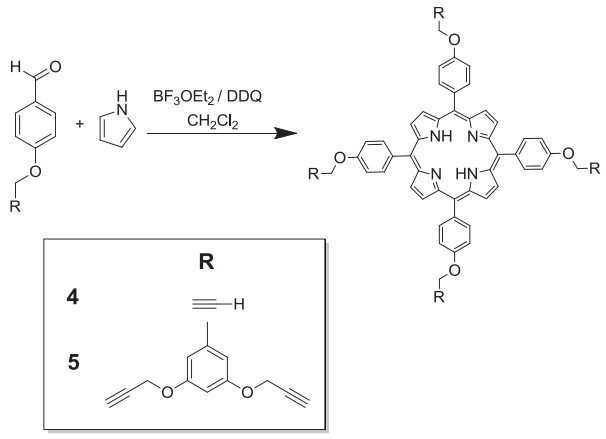


**Fig. 2.** Synthesis of *TPPh (2H) tetra-alkyne* **(4)** and *TPPh (2H) octa-alkyne* **(5)**.

chromatography using $CH_2Cl_2$ (100%) as eluent to give the product **(4)** as purple crystals (90.1 mg, 0.108 mmol). Yield: 14%.

$^1$H NMR (400 MHz, $CDCl_3$) (SI-Scheme 3) $\delta$ (ppm) = −2.75 (s, 2H), 2.70 (dd, $J$ = 3.09, 1.66 Hz, 4H), 4.98 (d, $J$ = 2.38 Hz 8H), 7.36 (dd, $J$ = 9.02, 2.30 Hz 8H), 8.22−8.08 (m, 8H), 8.89 (s, 8H).

$^{13}$C NMR (100 MHz, $CDCl_3$) (SI-Scheme 4) $\delta$ (ppm) = 56.17, 75.84, 78.68, 113.13, 119.56, 135.49, 135.56, 157.46.

*TPPh (2H) octa-alkyne* **(5)** was obtained using the same procedure described above (Fig. 2), employing 4-((3, 5-bis (prop-2-yn-1-yloxy)benzyl)oxy)benzaldehyde **(3)** (500 mg, 1.56 mmol), pyrrole (0.108 mL, 1.56 mmol), $BF_3OEt_2$ (0.02 mL, 0.16 mmol), DDQ (354 mg, 1.56 mmol) and $CH_2Cl_2$ (16 mL). The product was obtained as a purple solid (200 mg 0.136 mmol). Yield: 35%.

$^1$H NMR (400 MHz, $CDCl_3$) (SI-Scheme 5) $\delta$ (ppm) = 2.58 (t, $J$ = 2.39, 2.39 Hz, 8H), 4.78 (d, $J$ = 2.41 Hz, 16H), 5.32 (s, 8H), 6.68 (s, 1H), 6.91 (d, $J$ = 2.30 Hz, 4H), 7.35 (d, $J$ = 8.69 Hz, 8H), 8.12 (d, $J$ = 8.70 Hz, 8H), 8.86 (s, 8H), −2.74 (s, 2H).

$^{13}$C NMR (100 MHz, $CDCl_3$) (SI-Scheme 6) $\delta$ (ppm) = 56.04, 75.79, 78.35, 101.89, 107.05, 113, 131.93, 135.42, 139.72, 150.45, 158.32, 158.98.

### 2.3.4. Metallation of the porphyrin core

The metallation of the porphyrin core was carried out by dissolving the porphyrin in chloroform with further addition of zinc acetate in excess (Fig. 3). The progress of the reaction was monitored by TLC until the reaction was completed; after that, the reaction mixture was filtered and the product was employed without further purification.

*2.3.4.1. TPPh (Zn) tetra-alkyne* ***(6)***. TPPh (2H) tetra-alkyne **(3)** (0.76 g, 0.914 mmol) was dissolved in $CHCl_3$ (20 mL) until the solution was homogenous. Then, Zn $(OAc)_2$ (1.67 g, 9.14 mmol) was dissolved in MeOH (50 mL) and added to the reaction mixture, which was stirred overnight, filtered, washed with water, and dried with $Na_2SO_4$. The desired product was obtained as a purple solid (735 mg, 0.822 mmol). Yield: 90%.

$^1$H NMR (400 MHz, $CDCl_3$) (SI-Scheme 7): $\delta$ ppm = 2.70 (t, $J$ = 2.36, 2.36 Hz, 4H), 4.99 (d, $J$ = 2.33 Hz, 8H), 7.37 (d, $J$ = 8.35 Hz, 8H), 8.17−8.12 (m, 8H), 8.86 (s, 8H).

$^{13}$C NMR (100 MHz, $CDCl_3$) $\delta$ ppm 56.19, 75.82, 78.74, 113, 120.58, 131.93, 135.36, 136.09, 150.44, 157.31.

*2.3.4.2. TPPh (Zn) octa-alkyne* ***(7)***. This reaction was carried out employing the same procedure described above, in this case using TPPh (2H) octa-alkyne **(5)** (0.56 mg, 0.38 mmol) and $Zn(OAc)_2$ (0.698 g, 3.8 mmol). The desired product was obtained as a purple solid (525 mg 0.342 mmol). Yield: 90%.

$^1$H NMR (400 MHz, $CDCl_3$) (SI-Scheme 8) $\delta$ ppm = 2.58 (t, $J$ = 2.40, 2.40 Hz, 8H), 4.78 (d, $J$ = 2.40 Hz, 16H), 5.32 (s, 8H), 6.67 (t, $J$ = 2.29, 2.29 Hz, 4H), 6.91 (d, $J$ = 2.27 Hz, 8H), 7.35 (d, $J$ = 8.64 Hz, 8H), 8.97 (s, 8H), 8.13 (d, $J$ = 8.59 Hz, 8H).

$^{13}$C NMR (100 MHz, $CDCl_3$) $\delta$ (ppm): 56.04, 75.79, 78.35, 101.89, 107.05, 113, 131.93, 135.42, 139.72, 150.45, 158.32, 158.98.

### 2.3.5. Cholic acid azidation

The azidation of cholic acid was achieved according to the method reported by Pore et al. [37] and the synthetic sequence is illustrated in Fig. 4.

*2.3.5.1. Methyl 3α, 7α, 12α-trihydroxy-5β-cholan-24-ate* ***(8)***. Cholic acid (20 g, 48.9 mmol) was dissolved in methanol (100 mL) and $H_2SO_4$ (3 mL) was added as catalyst; the reaction mixture was heated at 80 °C for 3 h. Then, the solvent was removed under vacuum and the solid was extracted using ethyl acetate and water (1:1). The obtained product was used in the next step without further purification.

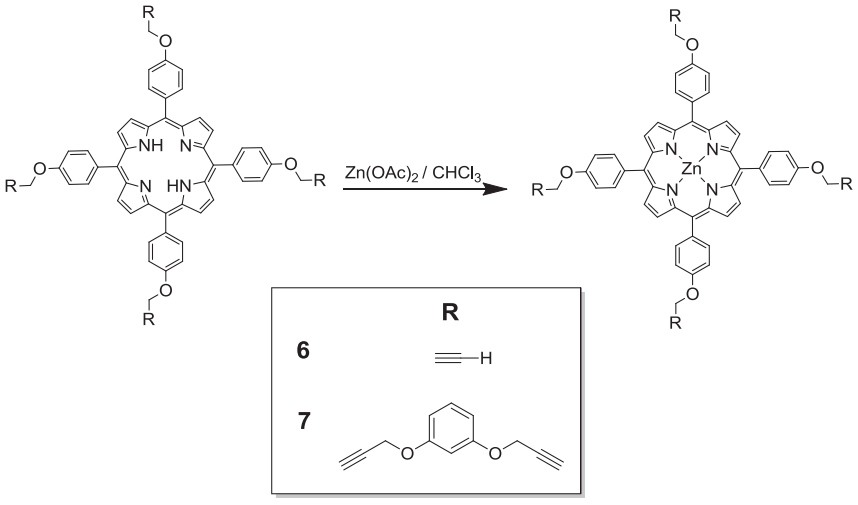


**Fig. 3.** Synthesis of *TPPh (Zn) tetra-alkyne* **(6)** and *TPPh (Zn) octa-alkyne* **(7)**.

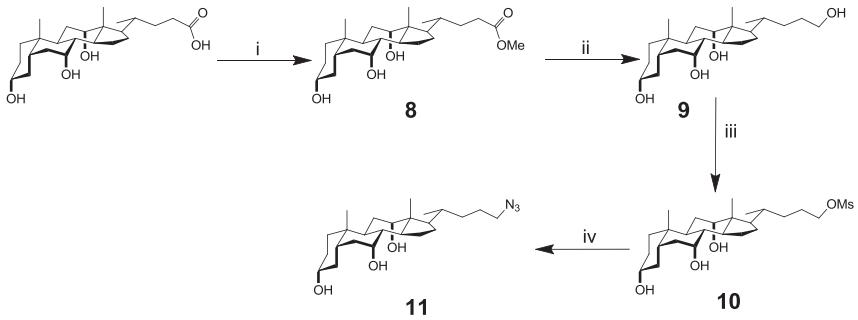


**Fig. 4.** Synthesis of *3α, 7α, 12α-Trihydroxy 24-azido-5β-cholane* **(11)**.

*2.3.5.2. 3α, 7α, 12α-Tetrahydroxy-5β-cholane **(9)**.* For the next step *Methyl 3α, 7α, 12α-trihydroxy-5β-cholan-24-ate* **(8)** (23 g, 54.5 mmol) was dissolved in THF at 0 °C. Afterwards, $LiAlH_4$ (10.34 g, 272.5 mmol) was added slowly and the mixture was stirred overnight. A mixture of water and ethyl acetate (4:2) was added slowly in order to quench the reaction and the mixture was stirred for 2 more hours. Then, it was filtered under vacuum and the product was purified by extraction using water, ethyl acetate and brine. The organic phase was concentrated at reduced pressure and the desired product was obtained as a white solid (19.9 g, 50.4 mmol). Yield: 92%.

$^1$H NMR (400 MHz, DMSO-$d_6$) $\delta$ ppm 3.24–3.13 (m, 1H), 3.65–3.58 (m, 1H), 3.83–3.76 (m, 1H), 4.31 (t, $J$ = 4.76, 4.76 Hz, 2H), 4.09 (d, $J$ = 3.61 Hz, 1H), 4.00 (d, $J$ = 3.42 Hz, 1H), 0.9 (d $J$ = *6.5 Hz* 3H) 0.60 (s, 3H), 0.81 (s, 3H).

*2.3.5.3. 3α, 7α, 12α-Trihydroxy 24-mesyloxy-5β-cholane **(10)**. 3α, 7α, 12α-Tetrahydroxy-5β-cholane* **(9)** (3 g, 7.6 mmol) was dissolved in pyridine and the solution was placed in an ice bath at 0 °C. Mesylchloride (0.6 mL, 7.6 mmol) was then slowly added and the reaction mixture was stirred for 30 min; then it was quenched with water. The product was extracted using water, ethyl acetate and brine. After that, the organic phase was concentrated under vacuum and the crude product was purified by column chromatography using ethyl acetate and hexanes (7:3). The desired product **(10)** was obtained as a white powder (500 mg, 1.05 mmol). Yield: 14%.

$^1$H NMR (400 MHz, $CDCl_3$) $\delta$ (ppm): 0.71 (s, 3H), 0.91 (s, 3H), 1.02–0.97 (m, 3H), 2.99 (d, $J$ = 0.88 Hz, 3H), 3.67–3.58 (m, 2H), 3.90–3.83 (m, 1H), 4.05–3.98 (m, 1H), 4.60–4.46 (m, 1H).

*2.3.5.4. 3α, 7α, 12α-Trihydroxy 24-azido-5β-cholane **(11)**. 3α, 7α, 12α-Trihydroxy 24-mesyloxy-5β-cholane* **(10)** (1 g, 2.38 mmol) was dissolved in dry DMF. Then, sodium azide (0.873 g, 13.4 mmol) was added and the reaction mixture was heated at 80 °C for 24 h. The product was isolated by extraction using water, ethyl acetate and brine. Afterwards it was purified by column chromatography using ethyl acetate and hexanes (6:4). The desired product **(11)** was obtained as a white powder (598 mg, 1.428 mmol). Yield: 60%.

$^1$H NMR (400 MHz, $CDCl_3$) (SI-Scheme 9) $\delta$ ppm = 0.70 (s, 3H), 0.93 (s, 3H), 1.0 (d, 3H), 3.62 (m, 2H), 3.86 (m, 1H), 3.9 (m, 1H), 4.01 (m, 1H).

*2.3.6. Synthesis of modified porphyrins*

After having obtained *TPPh (Zn) tetra-alkyne* **(7)**, *TPPh (Zn) octa-alkyne* **(8)** and the *3α, 7α, 12α-Trihydroxy 24-azido-5β-cholane* **(11)** we carried out the corresponding coupling reaction to obtain the final products: *TPPh (Zn) tetra-CA* **(12)** and *TPPh (Zn) octa-CA* **(13).**

*2.3.6.1. TPPh (Zn) tetra-CA **(12)**. TPPh (Zn) tetra-alkyne* **(7)** (200 mg, 0.2236 mmol) was added to a mixture of dry THF (2 mL) and $Et_3N$ (2 mL) to get a homogeneous solution. Then *3α,7α,12α-Trihydroxy 24-azido-5β-cholane* **(11)** (0.563 g, 1.34 mmol) and a catalytic amount of $CuBr(PPh_3)_3$ were added. The resulting reaction mixture was heated at 60 °C for 3 days; then the reaction was quenched. The crude product was obtained as a dark purple solid, which was washed with methanol, acetone, ethyl acetate, chloroform and dichloromethane. Finally the product (Fig. 5) was purified by column chromatography using $CH_2Cl_2$:MeOH (97:3) as eluent and concentrated at reduced pressure to give a purple solid (0.42 g, 0.16 mmol) Yield: 73%.

$^1$H NMR (400 MHz, DMSO-$d_6$) (SI-Scheme 10) $\delta$ ppm = 0.62 (s, 12H), 0.84 (s, 12H), 0.98–0.93 (m, 12H), 3.63–3.57 (m, 4H), 3.71–3.65 (m, 4H), 3.87–3.80 (m, 4H), 4.20–4.16 (m, 4H, OH), 4.29–4.25 (m, 4H, OH), 4.34–4.29 (m, 4H, OH), 5.48–5.37 (m, 8H), 7.49–7.42 (m, 8H), 8.10–8.05 (m, 8H), 8.49–8.46 (m, 4H), 8.79 (s, 8H).

$^{13}$C NMR (100 MHz, DMSO-$d_6$) (SI-Scheme 11) $\delta$ (ppm): 149.43, 142.27, 135.12, 131.45, 124.06, 119.83, 112.86, 79.10, 79.08, 71.02, 70.94, 66.18, 66.04, 61.43, 61.34, 61.29, 57.89, 48.52, 46.26, 45.69, 41.33, 36.85, 35.39, 34.01, 32.08, 31.8, 30.61, 29.22, 27.33, 26.11, 22.97, 17.36, 12.3.

MALDI-TOF-MS (SI-Scheme 12): *m/z*: calcd for $C_{152}H_{200}N_{16}O_{16}Zn$: 2572.69; found 2572.47 $[M+H]^+$.

*2.3.6.2. TPPh (Zn) octa-CA **(13)**.* TPPh (Zn) octa-alkyne **(8)** (100 mg, 0.0423 mmol) was dissolved in a mixture of dry THF (2 mL) and $Et_3N$ (2 mL). Then, *3α, 7α, 12α-Trihydroxy 24-azido-5β-cholane* **(11)** (0.1773 g, 0.423 mmol) and a catalytic amount of $CuBr(PPh_3)_3$ were added. The reaction mixture was heated at 60 °C for 5 days (Fig. 6). The crude product was purified by column chromatography using $CH_2Cl_2$:MeOH (97:3). Finally, the desired product was obtained as a purple solid (155 mg, 0.0317 mmol). Yield: 75%.

$^1$H NMR (400 MHz DMSO-$d_6$) (SI-Scheme 13) $\delta$ ppm = 0.56 (s, 24H), 0.77 (s, 24H), 0.94–0.91 (m, 24H), 3.65–3.60 (m, 8H), 3.83–3.77 (m, 8H), 4.17–4.10 (m, 8H), 4.24–4.19 (m, 8H, OH), 4.37–4.26 (m, 8H, OH), 4.70–4.64 (m, 8H, OH), 5.25–5.19 (m, 16H), 5.35–5.31 (m, 8H), 6.83–6.80 (m, 4H), 6.97–6.94 (m, 8H), 7.47–7.41 (m, 8H), 8.12–8.07 (m, 8H), 8.38–8.35 (m, 8H), 8.83–8.79 (m, 8H).

$^{13}$C NMR (100 MHz, DMSO-$d_6$) (SI-Scheme 14) $\delta$ (ppm):149.42, 142.05, 135.23, 131.72, 130.99, 124.01, 112.85, 107.08, 106.96, 70.98, 66.12, 61.39, 60.33, 56.27, 46.54, 45.32, 41.29, 36.82, 34.43, 31.83, 29, 26.16, 26.02, 24.14, 22.92, 22.64, 17.39, 12.36.

MALDI-TOF-MS (SI-Scheme 15): *m/z*: calcd for $C_{288}H_{396}N_{28}O_{36}Zn$: 4886.93; found 4890.72 $[M+H]^+$.

*2.3.7. Demetallation of TPPh (Zn) tetra-CA **(12)** and TPPh (Zn) octa-CA **(13)***

*2.3.7.1. TPPh (2H) tetra-CA **(14)**.* TPPh (Zn) tetra-CA **(12)** (61 mg, 0.0237 mmol) was dissolved in THF and a few drops of concentrated

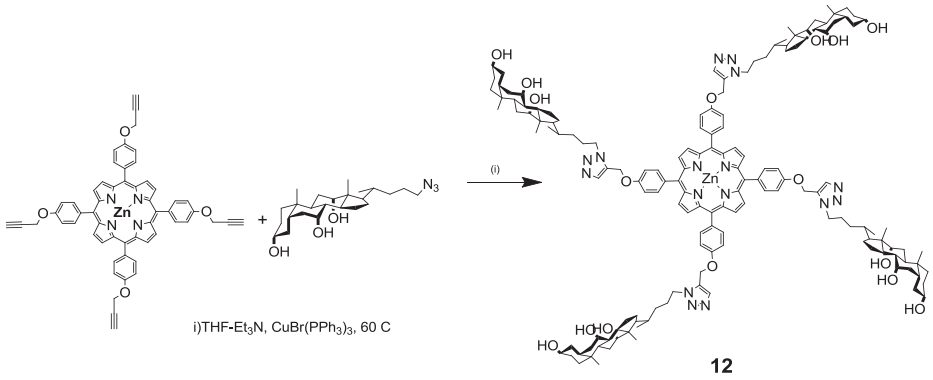


**Fig. 5.** Synthesis of TPPh (Zn) tetra-CA **(12)**.

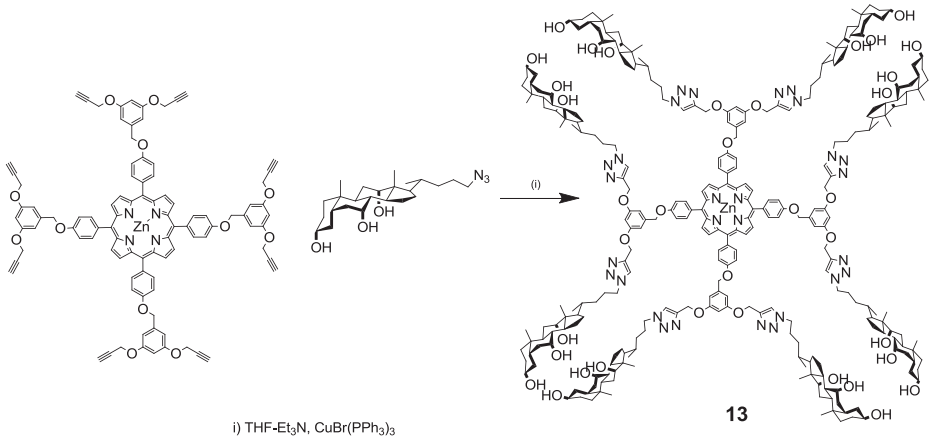


**Fig. 6.** Synthesis of TPPh (Zn) octa-CA **(13)**.

$H_3PO_4$ were added to the solution. The reaction mixture was stirred for 24 h (Fig. 7). Once the reaction was completed the product was isolated by biphasic extraction using THF and water; the extractions were repeated until the solution had a value of pH = 6 and the colour changed from green to purple. The organic phase was dried with $Na_2SO_4$ and concentrated under vacuum. The desired product was obtained as a purple solid (53.57 mg, 0.0213 mmol). Yield: 90%. $^1$H NMR (400 MHz, DMSO-$d_6$) (SI-Scheme 16) $\delta$ ppm −2.86 (m, 2H), 0.60 (m, 12H), 0.83 (m, 12H), 0.97–0.92 (m, 12H), 3.70–3.64 (m, 4H), 3.78–3.74 (m, 4H), 3.86–3.82 (m, 4H), 4.21–4.16 (m, 4H, OH), 4.29–4.25 (m, 4H, OH), 4.36–4.31 (m, 4H, OH), 5.47–5.41 (m, 8H), 7.53–7.46 (m, 8H), 8.16–8.10 (m, 8H), 8.50–8.47 (m, 4H), 8.8 (s, 8H).

MALDI-TOF-MS (SI-Scheme 17): *m/z:* calcd for $C_{152}H_{202}N_{16}O_{16}$: 2507.55; found 2510.86 $[M+H]^+$.

*2.3.7.2. TPPh (2H) octa-CA **(15)**.* TPPh (Zn) octa-CA **(13)** (50 mg, 0.0102 mmol) was treated under the same reaction conditions described above, using the same demetallation and purification methods (Fig. 8). The product was obtained as a purple solid (44.3 mg, 0.00919 mmol). Yield: 90%.

$^1$H NMR (400 MHz, DMSO-$d_6$) (SI-Scheme 18) $\delta$ (ppm) = −2.80 (m, 2H) 0.49–0.45 (m, 24 H), 0.71–0.66 (m, 24H), 0.92–0.86 (m,

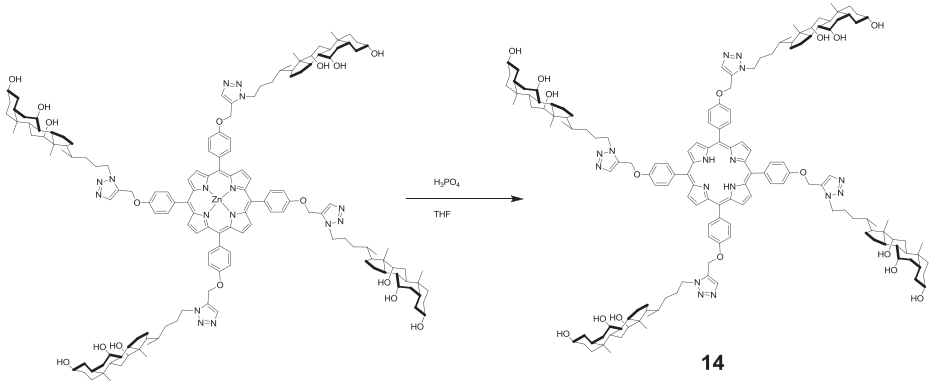


**Fig. 7.** Synthesis of TPPh (2H) tetra-CA **(14)**.

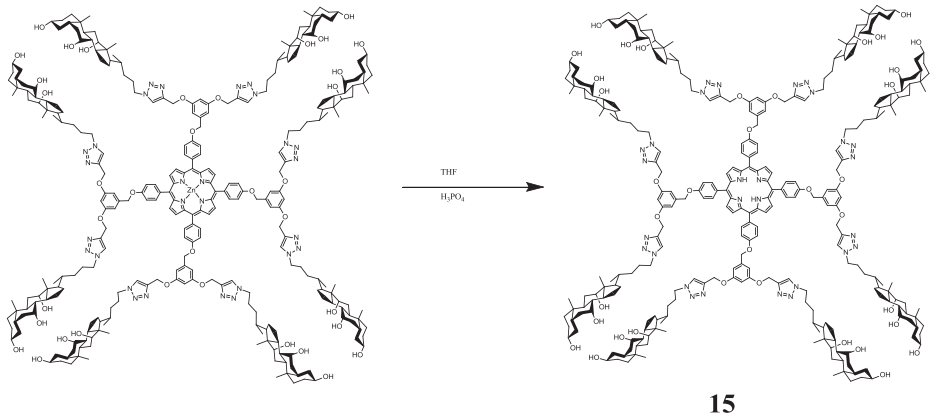


**Fig. 8.** Synthesis of TPPh (2H) octa-CA **(15).**

24H), 3.66–3.57 (m, 8H), 3.56–3.49 (m, 8H), 3.75–3.68 (m, 8H), 4.12–4.06 (m, 8H, OH), 4.19–4.12 (m, 8H, OH), 4.33–4.27 (m, 8H, OH), 5.23–5.19 (m, 16H), 5.35–5.32 (m, 8H), 6.80–6.78 (m, 4H), 6.96–6.95 (m, 8H), 7.47–7.44 (m, 8H), 8.14–8.11 (m, 8H), 8.35–8.33 (m, 8H), 8.86–8.82 (m, 8H).

MALDI-TOF-MS (SI-Scheme 19): *m/z*: calcd for $C_{288}H_{398}N_{28}O_{36}$: 4825.02; found 4849.67 $[M + H]^+$.

## 3. Results and discussion

The synthesis of four novel dendritic compounds bearing a porphyrin core and four or eight cholic acid units as peripheral groups was carried out successfully by the use of click chemistry. This approach consists on a series of azide-alkyne couplings, which allows the preparation of highly functionalized dendritic molecules under mild conditions. Furthermore, the demetallation was achieved from the corresponding metallated porphyrins in order to see the influence of the metal on the optical and photophysical properties.

### 3.1. Synthesis and characterization of the dendronized porphyrins

The dendronized porhyrins were synthesized as shown in Figs. 5–8. Firstly, the cholic acid unit was functionalized with multistep reactions to give a cholic acid derivative bearing a terminal azide group (**11**) (Fig. 4). This intermediate was further coupled in the presence of a functionalized porphyrin containing 4 and 8 terminal alkyne groups to give **12** and **13** (Figs. 5 and 6). The precursor porphyrins (**4** and **5**) were obtained by reacting 4 equiv of pyrrol in the presence of 4 equiv of the appropriate benzaldehyde derivative (Fig. 2). All the intermediates and final compounds prepared in this work were characterized by $^1H$ and $^{13}C$ NMR spectroscopy. The synthetic methods and the assignment of the NMR signals are described in detail in the Experimental Section.

The $^1H$ NMR spectrum of *4-(prop-2-1-yloxy)benzaldehyde* (**1**) shows the signal of the terminal alkyne proton at 2.57 ppm. However, for *4-((3,5-bis(prop-2-yn-1-yloxy)benzyl)oxy)benzaldehyde* (**2**) the terminal alkyne proton signal appears at 2.69 ppm, which confirms the structure of these intermediates.

In the case of the porphyrin *TPPh (2H) tetra-alkyne* **(3)** the NMR spectrum shows a singlet at 8.86 ppm due to the β-pyrrole protons, followed by two doublets at 8.15–8.13 and 7.37–7.34 ppm belonging to the *orto* and *meta* phenyl protons. In addition, a doublet at 4.98–4.97 ppm due to methylene groups, a triplet at 2.69 ppm corresponding to the terminal alkyne proton and a singlet at −2.75 ppm related to the porphyrin inner protons are also observed.

For porphyrin *TPPh (2H) octa-alkyne* **(4)** the structure was also confirmed by NMR spectroscopy. We observe a singlet at 8.86 ppm due the β-pyrrole protons, as well as a series of signals located at 8.13–8.10, 7.36–7.33, 6.91–6.90 and 6.68–6.66 ppm corresponding to the phenyl protons of the construct. A singlet at 5.31 ppm due to $CH_2$–O protons, followed by a doublet at 4.78–4.77 ppm belonging to the $CH_2$–C≡C protons, a triplet at 2.58 ppm corresponding to the C≡C–H protons and a singlet at −2.75 due to the porphyrin inner protons are also seen.

### 3.2. Metallation of the dendronized porphyrins

The metallation of the porphyrin core was carried out in the presence of Zn $(OAc)_2$ before the coupling reaction to avoid any complexation of the porphyrin core with copper derivatives, thereby obtaining the corresponding Zn-metallated compound [38]. In both compounds, *TPPh (Zn) tetra-alkyne* **(5)** and *TPPh (Zn) octa-alkyne* **(6)**, the insertion of the metal was confirmed by $^1H$ NMR spectroscopy due to the absence of the singlet arising from the inner protons of the free base porphyrin, which usually appear at −2.75 ppm.

Both dendronized porphyrins were obtained via click chemistry using azide-alkyne couplings. For this aim, we employed mild conditions that allow us to get a high functionalization of the porphyrin core, using a small amount of solvent with a simple purification.

In the $^1H$ NMR spectra of *TPPh (Zn) tetra-CA* **(12)** and *TPPh (Zn) octa CA* **(13)**, two spectral changes reveal the success in achieving the azide-alkyne coupling. The signal at 2.60 ppm due to the ≡C–H proton disappeared, whereas a new signal at 8.40 ppm due to the triazole protons appeared, thereby proving that the expected coupling occurred.

### 3.3. Demetallation of the dendronized porphyrins

Finally, *TPPh (Zn) tetra-CA* **(12)** and *TPPh (Zn) octa CA* **(13)** were demetallated (Figs. 7 and 8) to obtain the free-base derivatives *TPPh (2H) tetra-CA* (**14**) and *TPPh (2H) octa-CA* (**15**), respectively. The demetallation is confirmed by $^1H$ NMR spectroscopy by the appearance of the signal at −2.80 ppm (inner protons) and the remaining signal at 8.40 ppm of the triazole protons.

### 3.4. Optical properties of the dendronized porphyrins

The absorption spectra of the free base porphyrins *TPPh(2H)*

*tetra-CA* and *TPPh(2H) octa-CA* exhibited an intense absorption band (Soret band) at 421 nm, due to $S_0 \rightarrow S_2$ transition, followed by a series of low intensity bands (Q bands) at 517, 553, 594 and 651 nm (see Table 1) arising from the $S_0 \rightarrow S_1$ transition. On the other hand, the UV–vis spectra of branched metallated porphyrins, *TPPh(Zn) tetra-alkyne*, *TPPh(Zn) octa-alkyne*, *TPPh(Zn) tetra-CA* and *TPPh(Zn) octa-CA*, showed a Soret band at 426 nm, corresponding to the $S_0 \rightarrow S_2$ transition, followed by two Q bands at 559 and 599 nm, due to the $S_0 \rightarrow S_1$ transition. After metallation the absorption bands of the porphyrins showed a red shift compared to the non-metallated porphyrins. Moreover, Zn-metallated porphyrins exhibit two Q bands instead of four, because of their higher symmetry.

In the emission spectra of the free base porphyrins, two bands are observed at 650 and 721 nm due to the $S_1 \rightarrow S_0$ transition (see Table 1). By contrast, in the corresponding metallated porphyrins these bands appear at 605 and 650 nm, thereby showing a significant blue shift.

### 3.5. Aggregation in function of the polarity of the solvent

With the aim to study the effect of the polarity of the solvent on the self-assembly behaviour, we prepared 2 μM solutions of *TPPh (Zn) tetra-CA* **(12)** and *TPPh (Zn) octa-CA* **(13)** using THF as starting solvent, and the percentage of water varied from 0 to 70%; the aggregation was studied by monitoring the changes in the UV–vis spectra, the porphyrin concentration was kept in 2 μM (Fig. 9).

As soon as the polarity of the solvent increases, both metallated porphyrins, *TPPh (Zn) tetra-CA* **(12)** *and TPPh (Zn) octa-CA* **(13)** start to form J-aggregates, which is confirmed by a broadening of the Soret band of *TPPh (Zn) tetra-CA* **(12)**. In the case of *TPPh (Zn) octa-CA* **(13)**, a red shift of the Soret band from 427 to 433 nm is observed in both compounds. Moreover, the Q bands exhibit also a significant red shift from 558 to 664 nm.

### 3.6. Influence of triazole moieties

Similarly, to study how the presence of triazole units may affect the self-assembly behaviour of the metallated porphyrins, we prepared 2 μM solutions of *TPPh (Zn) tetra-alkyne* **(5)**, *TPPh (Zn) octa-alkyne* **(6)**, *TPPh (Zn) tetra-CA* **(12)**, and *TPPh (Zn) octa-CA* **(13)** under the conditions mentioned above, increasing gradually the quantity of water in order to see whether the J-aggregates are formed (Fig. 10).

In *TPPh (Zn) tetra-CA* **(12)** and *TPPh (Zn) octa-CA* **(13)**, the Soret band exhibits a red shift. In the case of *TPPh (Zn) tetra-CA* **(12)** the slight red is about 2 nm; the main difference is the spectral change in the Soret band shape, since in *TPPh (Zn) tetra-alkyne* **(6)** this band is sharp and well defined, whereas in porphyrin **(12)** the Soret band is broader, showing a shoulder which indicates the presence of J-aggregates [16]; in addition the Q bands show a red shift of 5 nm. On the other hand, *TPPh (Zn) octa-CA* **(13)** shows a red shift of 3 nm in the Soret band, compared to *TPPh (Zn) octa-alkyne* **(7)**. This band resulted to be broader and the Q bands exhibit also a red shift of 3 nm compared to porphyrin **(13)**. According to these results, it is possible to remark the influence of the triazole units in the self-assembly of the branched porphyrins in aqueous media. The presence of this moiety makes possible the formation of J-aggregates because of the possible interactions between triazole units with Zinc (II).

### 3.7. Effect of the metallation

The metallation of the branched porphyrins plays an important role in the formation of aggregates. To obtain a deeper insight, we have studied the metallated porphyrins (*TPPh (Zn) tetra-CA* **(12)** and *TPPh (Zn) octa-CA* **(13)**) as well as their free base analogues (*TPPh (2H) tetra-CA* **(14)** *and TPPh (2H) octa-CA* **(15)**) by absorption spectroscopy (Fig. 11).

It is well known that the interaction of zinc (II)-porphyrins with pyridine or imidazole tends to give a good association without spoiling the photoexcited-state dynamics of porphyrins [39,40]. The Soret band is the most affected, showing a broadening and a red shift due to the electron-withdrawing effect of the metal ion. In the Zn-metallated porphyrins, the Soret band also changes in shape due to the self-assembly process (aggregation) promoted by the triazole-zinc (II) interactions. As soon as we remove the Zinc (II) ions these interactions disappear and the self-assembly process do not occur, which can be detected by the shape and wavelength of the Soret band.

### 3.8. Effect of the temperature

The temperature is one of the main factors able to modify the self-assembly process, so that we decided to perform some experiments in order to monitor the formation of aggregates as a function of the temperature and to study thermal stability of the metallated porphyrins (Fig. 12).

It is worth noticing that in the absorbance spectra of *TPPh (Zn) tetra-CA* **(12)** and *TPPh (Zn) octa-CA* **(13)**, as soon as we increase the temperature, the Soret band exhibits significant changes in shape and shift. Enhancing the temperature provokes a disappearance of the Zn-porphyrin-triazole interactions, thereby causing a dissociation of the J-aggregates. This can be observed by the changes in shape and shift of the Soret band. In the case of *TPPh (Zn) tetra-CA* **(12)** once the temperature increased the shoulder of the Soret band vanished and the Soret band suffered a slight blue shift from 429 to 427 nm at 55 °C. On the contrary, upon the heating in the UV–vis spectrum of *TPPh (Zn) octa-CA* **(13)** the Soret band became narrower and exhibited a blue shift from 439 to 435 nm.

### 3.9. Effect of the aggregates on the emission

The comparison of the emission spectra of compounds TPPh(Zn) tetra-alkyne **(6)**, TPPh(Zn) tetra-CA **(12)** (Fig. 13), TPPh(Zn) octa-alkyne **(7)** and TPPh(Zn) octa-CA **(13)** (Fig. 14) confirms the

**Table 1**
Optical properties of the free base and metallated porphyrins in THF.

| Compound | Absorption λ (nm) | ε ($M^{-1}$ $cm^{-1}$ at) | Cut off (nm) | Emission λ (nm) | Cut off (nm) |
|---|---|---|---|---|---|
| TPPh (Zn) tetra-alkyne | 426, 559, 598 | 274,069 | 650 | 605, 658 | 750 |
| TPPh (Zn) octa-alkyne | 426, 557, 599 | 474,232 | 650 | 614, 656 | 750 |
| TPPh (Zn) tetra-CA | 426, 558, 599 | 550,220 | 650 | 608, 659 | 750 |
| TPPh (Zn) octa-CA | 427, 557, 598 | 306,029 | 650 | 615, 655 | 750 |
| TPPh (2H) tetra-CA | 421, 517, 553, 594, 651 | 342,026 | 700 | 657, 721 | 800 |
| TPPh (2H) octa-CA | 421, 519, 554, 594, 651 | 516,988 | 700 | 654, 719 | 800 |

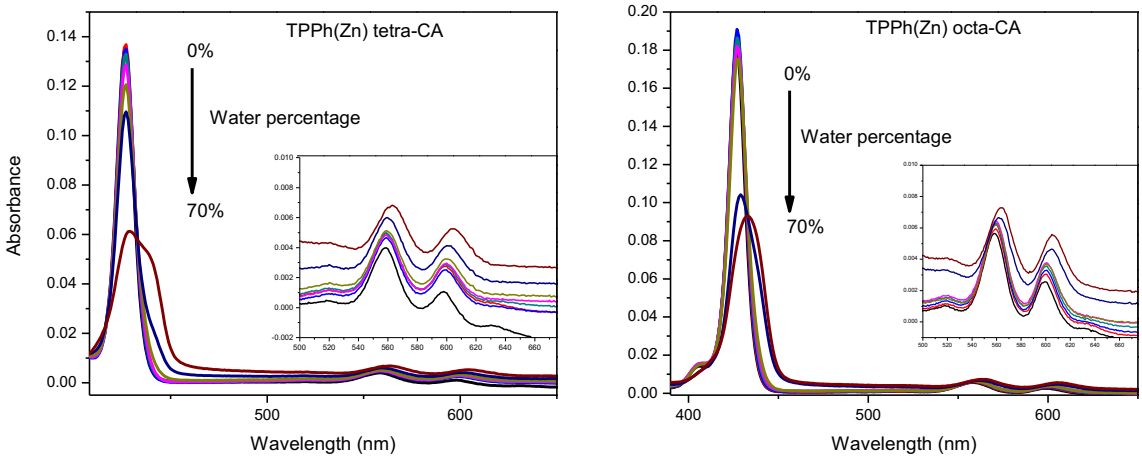


**Fig. 9.** UV–vis spectra of the TPPh (Zn) tetra-CA and TPPh (Zn) octa-CA recorded in different THF: water mixtures: (100:0; 90:10; 80:20; 70:30; 60:40; 50:50; 40:60 and 30:70) at room temperature (conc = 2 μM).

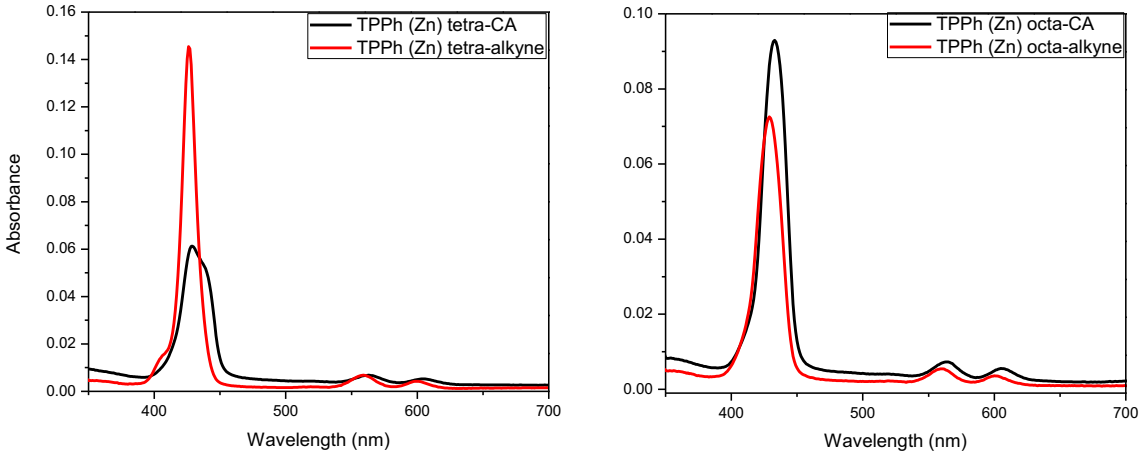


**Fig. 10.** Triazole moieties and J-aggregate assembly dependence in THF: water (30:70) media at room temperature (conc = 2 μM).

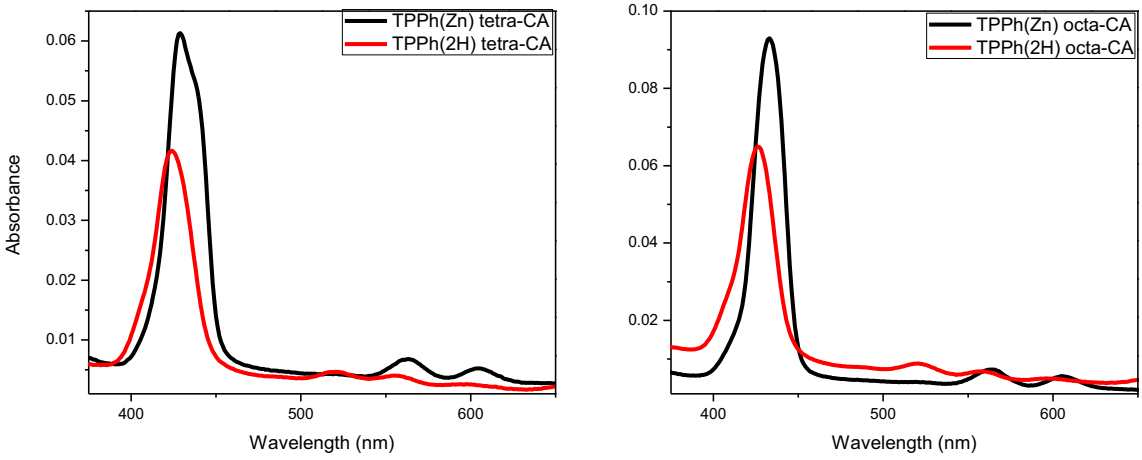


**Fig. 11.** Influence of the metallation on the formation of J-aggregates recorded in THF: water (30:70) media at room temperature (conc = 2 μM).

formation of porphyrin aggregates in THF:water and THF: hexane solutions [41].

As we can see, TPPh(Zn) tetra-alkyne (Fig. 13 right) shows the typical emission spectrum of a porphyrin in THF (black line). However, as soon as we change the polarity of the media, using mixtures THF:water 30:70 (red line), THF:Hexane 30:70 (blue line) and THF:chloroform 30:70 (magenta line) we can observe significant changes in the intensity of the emission bands, due to the

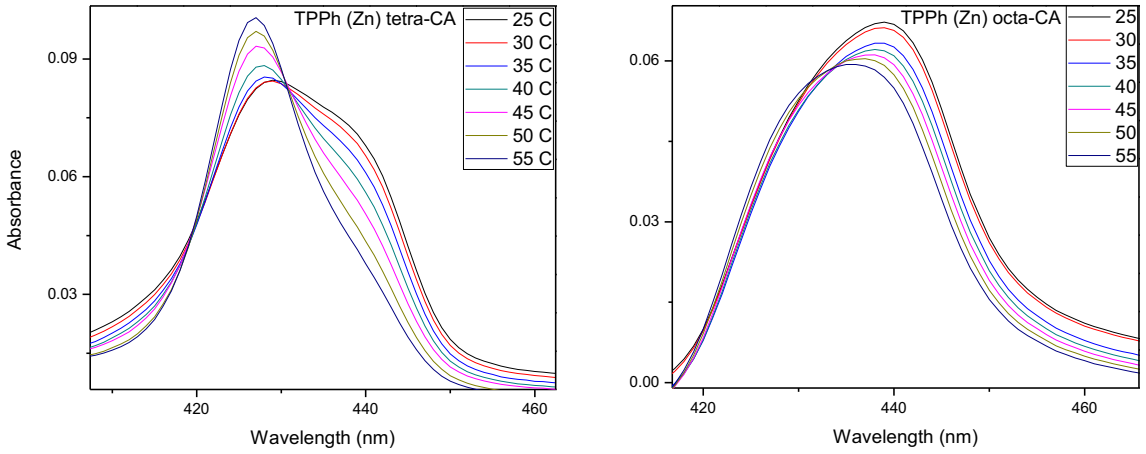


**Fig. 12.** Temperature dependence in the J-aggregate assembly recorded in THF:water (30:70) at room temperature (conc = 2 μM).

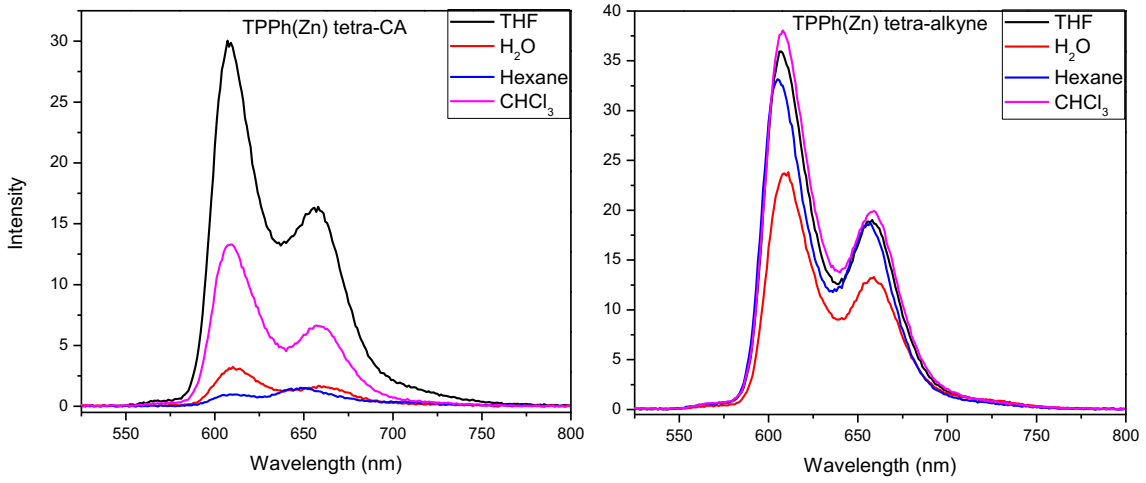


**Fig. 13.** Emission spectra of TPPh(Zn) tetra-CA (left) and TPPh(Zn) tetra-alkyne (right) in THF:water 30:70 (red line), THF:hexanes 30:70 (blue line), THF:$CHCl_3$ 30:70 (magenta line) and THF (black line) at room temperature (conc = 2 μM). (For interpretation of the references to colour in this figure legend, the reader is referred to the web version of this article.)

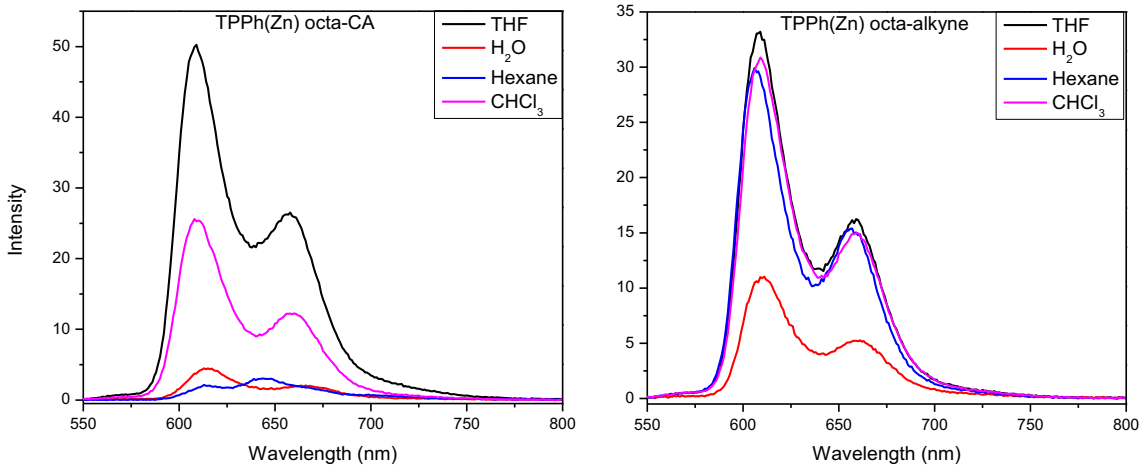


**Fig. 14.** Emission spectra of TPPh(Zn) octa-CA (left) and TPPh(Zn) octa-alkyne (right) in THF:water 30:70 (red line), THF:hexanes 30:70 (blue line), THF:$CHCl_3$ 30:70 (magenta line) and THF (black line) at room temperature (conc = 2 μM). (For interpretation of the references to colour in this figure legend, the reader is referred to the web version of this article.)

formation of aggregates, which are less emissive.

When we performed the same experiments with TPPh(Zn) tetra-CA (Fig. 13 left) this compound exhibited a typical behaviour in THF, however, the emission spectra changed drastically in shape and intensity in THF:water 30:70 (red line), THF:Hexane 30:70 (blue line) and THF:chloroform 30:70 (magenta line). It is worth to

point out that in THF:water 30:70 and THF:hexane 30:70 this compound showed a significant quenching in the emission bands, arising from the formation of the aggregates. A similar behaviour has been reported for other similar porphyrinic compounds, whose aggregates showed poor emission intensity [41].

The emission spectra of compounds TPPh(Zn) octa-CA and TPPh(Zn) octa-alkyne are shown in Fig. 14, left and right, respectively. A similar behaviour has been also observed in these systems, which confirmed the formation of aggregates as in the previous case.

## 4. Conclusion

A new series of dendronized porphyrins containing cholic acid units were synthesized and characterized. The absorption and emission spectra show the characteristic bands of the porphyrin core which are not significantly affected by the presence of the cholic acid units. These compounds exhibit the typical Soret absorption of the porphyrin at ca. $\lambda = 421$ nm followed by four Q bands between 500 and 700 nm. After metallation, the Soret band red-shifts to ca. $\lambda = 421$ nm and only two Q bands are observed. The free base porphyrins show emission at ca. $\lambda = 657$ and 721 nm whereas after metallation these bands are blue-shifted to ca. $\lambda = 605$ and 658 nm. The aggregation phenomenon was studied as a function of factors such as the polarity of the solvent, temperature, metallation and presence of the triazole rings. Increasing the polarity of the solvent gives rise to the formation of J-aggregates. On the other hand the metallated porphyrins containing triazole units favour the formation of intramolecular J-aggregates due to the triazole-zinc (II) interactions. Enhancing the temperature provokes a disappearance of the Zn-porphyrin-triazole interactions, thereby causing a dissociation of the J-aggregates.

## Acknowledgements

We thank María de los Ángeles Peña González, Elizabeth Huerta Salazar, Gerardo Cedillo, Louiza Mahrouche and Marie-Christine Tang for their assistance in the characterization of all the compounds. We are also grateful to CONACYT (Projects 128788 and 253155), PAPIIT (Project IN-100316) and NSERC Canada. EAO thanks Posgrado en Ciencias Químicas UNAM, and CONACYT for scholarship and Ph.D. Grant (223409).

## Appendix A. Supplementary data

Supplementary data related to this article can be found at http://dx.doi.org/10.1016/j.dyepig.2016.04.047.

## References

[1] Senge BMO, Fazekas M, Notaras EGA, Blau WJ, Zawadzka M, Locos OB. Nonlinear optical properties of porphyrins. Adv Mater 2007;19:2737–74. http://dx.doi.org/10.1002/adma.200601850.
[2] Suijkerbuijk BM, Gebbink RJ. Merging porphyrins with organometallics : synthesis and applications. Angew Chem Int Ed Engl 2008;47:7396–421. http://dx.doi.org/10.1002/anie.200703362.
[3] Anderson HL. Building molecular wires from the colours of life : conjugated porphyrin oligomers. Chem Commun 1999:2323–30. http://dx.doi.org/10.1039/A904209A.
[4] Auwärter W, Écija D, Klappenberger F, Barth JV. Porphyrins at interfaces. Nat Chem 2015;7:105–20. http://dx.doi.org/10.1038/nchem.2159.
[5] Gottfried JM. Surface chemistry of porphyrins and phthalocyanines. Surf Sci Rep 2015;70:259–379. http://dx.doi.org/10.1016/j.surfrep.2015.04.001.
[6] Imaoka T, Horiguchi H, Yamamoto K. Metal assembly in novel dendrimers with porphyrin cores. J Am Chem Soc 2003;125:340–1. http://dx.doi.org/10.1021/ja0285060.
[7] Yan X, Goodson T, Imaoka T, Yamamoto K. Up-converted emission in a series of phenylazomethine dendrimers with a porphyrin core. J Phys Chem B 2005;109:9321–9. http://dx.doi.org/10.1021/jp044105q.
[8] Zaragoza-Galán G, Fowler MA, Duhamel J, Rein R, Solladie N, Rivera E. Synthesis and characterization of novel pyrene-dendronized porphyrins exhibiting efficient fluorescence resonance energy transfer: optical and photophysical properties. Langmuir 2012;28:11195–205. http://dx.doi.org/10.1021/la301284v.
[9] Zaragoza-Galán G, Fowler M, Rein R, Solladie N, Duhamel J, Rivera E. Fluorescence resonance energy transfer in partially and fully labeled pyrene dendronized porphyrins studied with model free analysis. J Phys Chem C 2014;118:8280–94. http://dx.doi.org/10.1021/jp501445n.
[10] Caicedo C, Zaragoza-Galán G, Crusats J. Design of novel luminescent porphyrins bearing donor–acceptor groups. J. Porphyr Phthalocyanines 2014;18:209–20. http://dx.doi.org/10.1142/S1088424613501083.
[11] Davis AP. Anion binding and transport by steroid-based receptors. Coord Chem Rev 2006;250:2939–51. http://dx.doi.org/10.1016/j.ccr.2006.05.008.
[12] Vollmer MS, Effenberger F, Stu T, Hartschuh A, Port H, Wolf HC. Steroid-bridged anthryloligothienylporphyrins : synthesis and study on the intramolecular energy transfer. J Org Chem 1998;63:5080–7. http://dx.doi.org/10.1021/jo980251e.
[13] Kolb HC, Finn MG, Sharpless KB. Click chemistry: diverse chemical function from a few good reactions. Angew Chem Int Ed 2001;40:2004–21. http://dx.doi.org/10.1002/1521-3773(20010601)40:11<2004::AID-ANIE2004>3.0.CO;2–5.
[14] Leonardi MJ, Topka MR, Dinolfo PH. Efficient förster resonance energy transfer in 1,2,3-triazole linked bodipy-zn(ii) meso-tetraphenylporphyrin donor–acceptor arrays. Inorg Chem 2012;51:13114–22. http://dx.doi.org/10.1021/ic301170a.
[15] Nguyen NT, Hofkens J, Scheblykin IG, Kruk M, Dehaen W. Click reaction synthesis and photophysical studies of dendritic metalloporphyrins. Eur J Org Chem 2014;8:1766–77. http://dx.doi.org/10.1002/ejoc.201301158.
[16] Scheibe VII G. Fachgebiet photochemie und photographische chemie. Angew Chem 1936;49:562–4. http://dx.doi.org/10.1002/ange.19360493110.
[17] Scheibe G. Herstellung von Futterhefen aus Sulfitablaugen. Angew Chem 1937;50:51. http://dx.doi.org/10.1002/ange.19370500113.
[18] Jelley EE. Molecular, nematic and crystal states of I: I-diethyl—cyanine chloride. Nature 1937;139:631–2. http://dx.doi.org/10.1038/139631b0.
[19] Verma S, Ghosh A, Das A, Ghosh NH. Ultrafast exciton dynamics of j- and h-aggregtes of the porphyrin-catechol in aqueous solution. J Phys Chem B 2010;114:8327–34. http://dx.doi.org/10.1021/jp101643c.
[20] Schenning APHJ, Meijer EW. Supramolecular electronics; nanowires from self-assembled p-conjugated systems. Chem Commun 2005:3245–58. http://dx.doi.org/10.1039/B501804H.
[21] Konigstein C, Bauer R. Photoinduced hydrogen production in dilute solutions and organized assemblies. Int J Hydrogen Energy 1993;18:735–41. http://dx.doi.org/10.1016/0360-3199(93)90152-Z.
[22] Liu S, Wang MW, Briseno LA, Mannsfeld BCS, Bao Z. Controlled deposition of crystalline organic semiconductors for field-effect-transistor applications. Adv Mater 2009;21:1217–32. http://dx.doi.org/10.1002/adma.200802202.
[23] Salomon A, Genet C, Ebbensen WT. Molecule-light complex: dynamic of hybrid molecule-surface plasmon states. Angew Chem Int Ed 2009;121:8904–7. http://dx.doi.org/10.1002/ange.200903191.
[24] Vacha M, Furuki M, Pu SL, Hashizume K, Tani T. Individual J-aggregate nanostructures as self-assembled organic microcavities. J Phys Chem B 2001;105:12226–9. http://dx.doi.org/10.1021/jp011360r.
[25] Zhao Y, Thorkelsson K, Mastroianni JA, Schilling T, Luther MJ, Rancatore JB, et al. Small-molecule-directed nanoparticle assembly towards stimuli-responsive nanocomposites. Nat Mater 2009;8:979–85. http://dx.doi.org/10.1038/nmat2565.
[26] D'Urso A, Fragalá ME, Purrello R. From self-assembly to noncovalent synthesis of programable porphyrins arrays in aqueous solution. Chem Commun 2012;48:8165–76. http://dx.doi.org/10.1039/c2cc31856c.
[27] Egawa Y, Hayashida R, Anazai J. pH-induced interconversion between J-aggregates and H-aggregates of 5, 10, 15, 20-tetrakis (4-sulfonatophenyl) porphyrin in polyelectrolyte multilayer films. Langmuir 2007;23:13146–50. http://dx.doi.org/10.1021/la701957b.
[28] Arai Y, Segawa H. Cl- complexation induced H- and J-aggregation of meso-tetrakis (4-sulfonatothienyl) porphyrin diacid in aqueous solution. J Phys Chem B 2011;115:7773–80. http://dx.doi.org/10.1021/jp2018428.
[29] Shirakawa M, Kawano S, Fujita N, Sada K, Shinkai S. Hydrogen-bond-assisted control of h versus j aggregation mode of porphyrins stacks in an organogel system. J Org Chem 2003;68:5037–44. http://dx.doi.org/10.1021/jo0341822.
[30] Bhosale VS, Kalyankar BM, Nalage VS, Lalander HC, Bhosale VS, Langford SJ, et al. pH dependent molecular self-assembly of octaphosphonate porphyrin of nanoscale dimensions: nanosphere and nanorod aggregates. Int J Mol Sci 2011;12:1464–73. http://dx.doi.org/10.3390/ijms12031464.
[31] Okada S, Segawa H. Substituent-control exciton in J-aggregates of protonated water-insoluble porphyrins. J Am Chem Soc 2003;125:2792–6. http://dx.doi.org/10.1021/ja017768j.
[32] Stephanek P, Dukh M, Saman D, Moravcova J, Kniezo L, Monti D, et al. Synthesis and solvent driven self-aggregation studies of meso-C-glycoside-porphyrin derivatives. Org Biomol Chem 2007;5:960–70. http://dx.doi.org/10.1039/B616096D.
[33] Ribo JM, Bofill JM, Crusats J, Rubires R. Point-Dipole approximation of the exciton coupling model versus type of bonding and excitons in porphyrin supramolecular structures. Chem Eur J 2001;7:2733–7. http://dx.doi.org/10.1002/1521-3765(20010702)7:13<2733::AID-CHEM2733>3.0.CO;2-Q.

[34] Micali N, Mallamace F, Castriciano M, Romeo A, Scolaro ML. Separation of scattering and absorption contributions in UV/visible spectra of resonant systems. Anal Chem 2001;73:4958–63. http://dx.doi.org/10.1021/ac010379n.
[35] Villari V, Mineo P, Scamporrino E, Micali N. Role of the hydrogen-bond in porphyrin J-aggregates. RSC Adv 2012;2:12989–98. http://dx.doi.org/10.1039/C2RA22260D.
[36] Lindsey JS, Schreiman CI, Hsu CH, Kearney CP, Marguerettaz MA. Rothemund and Adler-Longo reactions revisited: synthesis of tetraphenylporphyrins under equilibrium conditions. J Org Chem 1987;52:827–36. http://dx.doi.org/10.1021/jo00381a022.
[37] Pore SV, Aher GN, Kumar M, Shukla KP. Design and synthesis of fluconazole/bile acid conjugate using click reaction. Tetrahedron 2006;62:11178–86. http://dx.doi.org/10.1016/j.tet.2006.09.021.
[38] Okada M, Kishibe Y, Ide K, Takahashi T, Hasegawa T. Convenient approach to octa-glycosylated porphyrins via “click chemistry”. Int J Carbohydr Chem 2009;2009:1–9. http://dx.doi.org/10.1155/2009/305276.
[39] Maeda C, Kim P, Cho S, Park KJ, Lim MJ, Kim D, et al. Large porphyrin squares from the self-assembly of meso-traizole-appenden L-shaped meso-meso-linked Zn (II)-triporphyrins: synthesis and efficient energy transfer. Chem Eur J 2010;16:5052–61. http://dx.doi.org/10.1002/chem.200903195.
[40] Roberts AD, Schmidt WT, Crossley JM, Perrier S. Tunable self-assembly of triazole-linked porphyrin-polymer conjugates. Chem Eur J 2013;19:12759–70. http://dx.doi.org/10.1002/chem.201301133.
[41] Esch JH, Feiters MC, Peters AM, Nolte JM. UV-Vis, fluorescence, and EPR studies of porphyrins in bilayers of dioctadecyldimethylammonium surfactants. J Phys Chem 1994;98:5541–51. http://dx.doi.org/10.1021/j100072a022.